

## Specific Phosphopeptide Enrichment with Immobilized Titanium Ion Affinity Chromatography Adsorbent for Phosphoproteome Analysis

Houjiang Zhou,<sup>#</sup> Mingliang Ye,<sup>#</sup> Jing Dong, Guanghui Han, Xinning Jiang, Renan Wu, and Hanfa Zou\*

National Chromatographic R&A Center, Dalian Institute of Chemical Physics, Chinese Academy of Sciences, Dalian 116023, China

Received March 25, 2008

The elucidation of protein post-translational modifications, such as phosphorylation, remains a challenging analytical task for proteomic studies. Since many of the proteins targeted for phosphorylation are low in abundance and phosphorylation is typically substoichiometric, a prerequisite for their identification is the specific enrichment of phosphopeptide prior to mass spectrometric analysis. Here, we presented a new method termed as immobilized titanium ion affinity chromatography ( $\text{Ti}^{4+}$ -IMAC) for enriching phosphopeptides. A phosphate polymer, which was prepared by direct polymerization of monomers containing phosphate groups, was applied to immobilize  $\text{Ti}^{4+}$  through the chelating interaction between phosphate groups on the polymer and  $\text{Ti}^{4+}$ . The resulting  $\text{Ti}^{4+}$ -IMAC resin specifically isolates phosphopeptides from a digest mixture of standard phosphoproteins and nonphosphoprotein (BSA) in a ratio as low as 1:500.  $\text{Ti}^{4+}$ -IMAC was further applied for phosphoproteome analysis of mouse liver. We also compared  $\text{Ti}^{4+}$ -IMAC to other enrichment methods including  $\text{Fe}^{3+}$ -IMAC,  $\text{Zr}^{4+}$ -IMAC,  $\text{TiO}_2$  and  $\text{ZrO}_2$ , and demonstrate superior selectivity and efficiency of  $\text{Ti}^{4+}$ -IMAC for the isolation and enrichment of phosphopeptides. The high specificity and efficiency of phosphopeptide enrichment by  $\text{Ti}^{4+}$ -IMAC mainly resulted from the flexibility of immobilized titanium ion with spacer arm linked to polymer beads as well as the specific interaction between immobilized titanium ion and phosphate group on phosphopeptides.

**Keywords:** Immobilized metal ion affinity chromatography • titanium ion • phosphate polymer • phosphopeptide enrichment • phosphoproteome analysis

### Introduction

The diversity of distinct covalent forms of proteins greatly exceeds the number of proteins predicted by DNA coding capacities owing to directed post-translational modifications.<sup>1</sup> Reversible protein phosphorylation is among the most widespread post-translational modifications (PTM) in nature and has a vital role in regulating many complex biological processes such as cellular growth, division and signaling transduction.<sup>2</sup> Furthermore, it is estimated that one-third of all proteins is phosphorylated *in vivo* in mammalian cells at any time point.<sup>3</sup> Because of the importance of protein phosphorylation, so far, various methods for protein phosphorylation site mapping have been developed. However, this task remains a technical challenge, and there is an intense interest in development of new technologies and methods for studying phosphorylation events.<sup>4,5</sup>

Mass spectrometry (MS) and in particular tandem MS in combination with low-energy collision induced dissociation has become a powerful tool for characterization of covalent protein

modifications, including global profiling and quantification of protein phosphorylation.<sup>6,7</sup> For the MS-based methods, the phosphorylated protein is typically digested into peptides, and phosphopeptides are selectively isolated prior to mass spectrometry analysis to avoid the interference of huge amount of nonphosphopeptides, and subsequently fragmented in a mass spectrometer to assign the sequence and localize phosphorylation sites.<sup>8</sup> To date, various methods have been developed for selective enrichment of phosphopeptides. These selective methods can be classified into three main categories: (1) immunoprecipitation using serine/threonine- or tyrosine-specific antibodies,<sup>9,10</sup> which is limited by the antibody specificity and more costly; (2) chemical modification through  $\beta$ -elimination/concurrent Michael addition with using affinity tag to substitute the phosphate group on phosphopeptides,<sup>11–13</sup> which is labor-intensive and also suffers from sample loss caused by the multiple reaction steps and increased sample complexity by unavoidable side reactions; (3) specific interaction with adsorbents such as metal oxides ( $\text{TiO}_2$ ,  $\text{ZrO}_2$  and  $\text{Al}_2\text{O}_3$ ),<sup>14–24</sup> immobilized metal ion (usually  $\text{Fe}^{3+}$ ,  $\text{Ga}^{3+}$ ,  $\text{Ni}^{2+}$  and  $\text{Zr}^{4+}$ )<sup>25–32</sup> affinity chromatography adsorbents (IMAC), and strong ion exchange chromatography adsorbents.<sup>33–36</sup> Among these approaches, IMAC is the most commonly used to isolate phosphopeptides.

\* To whom correspondence should be addressed. Prof. Dr. Hanfa Zou, National Chromatographic R&A Center, Dalian Institute of Chemical Physics, Chinese Academy of Sciences, Dalian 116023, China. E-mail, hanfazou@dicp.ac.cn; tel, +86-411-84379610; fax, +86-411-84379620.

<sup>#</sup> Both authors contributed equally to this work.

Adsorbents with two types of chelating ligands, that is, iminodiacetic acid (IDA, a tridentate metal-chelator)<sup>37</sup> and nitrilotriacetic acid (NTA, a quadridentate metal-chelator)<sup>30,38,39</sup> are typically used for immobilization of  $\text{Fe}^{3+}$ ,  $\text{Ga}^{3+}$  or  $\text{Ni}^{2+}$  via chelating to the carboxylic groups and amino groups on IDA or NTA ligands in conventional IMAC. It is well-known that every NTA ligand binds to four of the six  $\text{Fe}^{3+}$ ,  $\text{Ga}^{3+}$  or  $\text{Ni}^{2+}$  coordination sites leaving two free sites for phosphopeptide binding, and every IDA ligand binds to three of the six  $\text{Fe}^{3+}$ ,  $\text{Ga}^{3+}$  or  $\text{Ni}^{2+}$  coordination sites leaving three sites for phosphopeptide binding. Each metal ion only coordinates one NTA ligand or IDA ligand, which may result in loss of the bound metal ions during sample loading and washing. Another weakness of IMAC using  $\text{Fe}^{3+}$ ,  $\text{Ga}^{3+}$  or  $\text{Ni}^{2+}$  is the nonspecific adsorption of acidic peptides and peptides containing histidine<sup>38–40</sup> because it binds not only phosphate groups, but also the carboxylic groups on the phosphopeptides, which certainly leads to reduce their specificity for enrichment of phosphopeptides.<sup>41</sup> One approach by blocking the acidic residues using methyl esterification<sup>42–45</sup> has been shown to enhance the specificity of phosphopeptide binding; the low yield of derivatization and the side reactions comprise the sensitivity of this method and increases the complexity of the sample. In the enrichment of phosphopeptides by metal oxides ( $\text{TiO}_2$  and  $\text{ZrO}_2$ ), considerable efforts by introducing hydroxy acids such as DHB,<sup>14,15</sup>  $\beta$ -hydroxypropanoic acid,<sup>46</sup> phthalic acid,<sup>47</sup> ammonium glutamate<sup>48</sup> and glutamic acid<sup>49</sup> in the loading and washing buffer have been made to improve the specificity of phosphopeptide enrichment.

In metal(IV) phosphonate chemistry such as Zr or Ti ions, it is well-known that the layer structure of metal phosphonate can be obtained by  $\text{MO}_6$  octahedra, and each Zr or Ti sharing six oxygen atoms with different monohydrogen phosphate groups. In turn, each monohydrogen phosphate group behaves as a tridentate anionic ligand and shares three oxygen atoms with three different metal atoms.<sup>50</sup> So, each metal ion coordinates to more than one phosphate molecule and the phosphates bind to more than one metal ion. Therefore, the extremely strong binding of the zirconium ions or titanium ions stack the original monolayer and provides a very stable, well-defined interface of metal phosphonate sites, where the metal ions located on the surface are very active and readily react when exposed to other phosphate group to bind them to the surface.<sup>51</sup> It is reasonable to think that if  $\text{Zr}^{4+}$  or  $\text{Ti}^{4+}$  is immobilized onto material with its surface containing phosphate group as ligands, the resulting IMAC adsorbents should also be able to bind phosphopeptides. In addition, the unique coordination specificity of Zr or Ti ions immobilized on the phosphate materials may also greatly improve the selectivity of phosphopeptide binding, which prevents from acidic peptides binding. The immobilization of  $\text{Zr}^{4+}$  for phosphopeptide enrichment was recently realized in our laboratory.<sup>4,52,53</sup> It was found that the prepared  $\text{Zr}^{4+}$ -IMAC has much higher specificity for phosphopeptides than conventional  $\text{Fe}^{3+}$ -IMAC does. In this study, we presented the adsorbent qualities of  $\text{Ti}^{4+}$ -IMAC for the enrichment of phosphopeptides. The porous phosphate polymer material used for immobilization of  $\text{Ti}^{4+}$  was prepared by direct copolymerization of a monomer containing phosphate group with cross-linker in the presence of porogenic solvents. After the polymer material was ground into beads, titanium ions were immobilized by incubating the polymer beads with  $\text{Ti}(\text{SO}_4)_2$  solution. We optimized the phosphopeptide enrichment procedures of  $\text{Ti}^{4+}$ -IMAC by using the tryptic peptide mixtures of some model proteins as the samples and

further evaluated its performance using the digests of mouse liver lysates. Some established isolation methods such as  $\text{Fe}^{3+}$ -IMAC,  $\text{Zr}^{4+}$ -IMAC,  $\text{TiO}_2$  and  $\text{ZrO}_2$  were also systematically compared with  $\text{Ti}^{4+}$ -IMAC for their specificity and efficiency and found that the  $\text{Ti}^{4+}$ -IMAC was the most efficient.

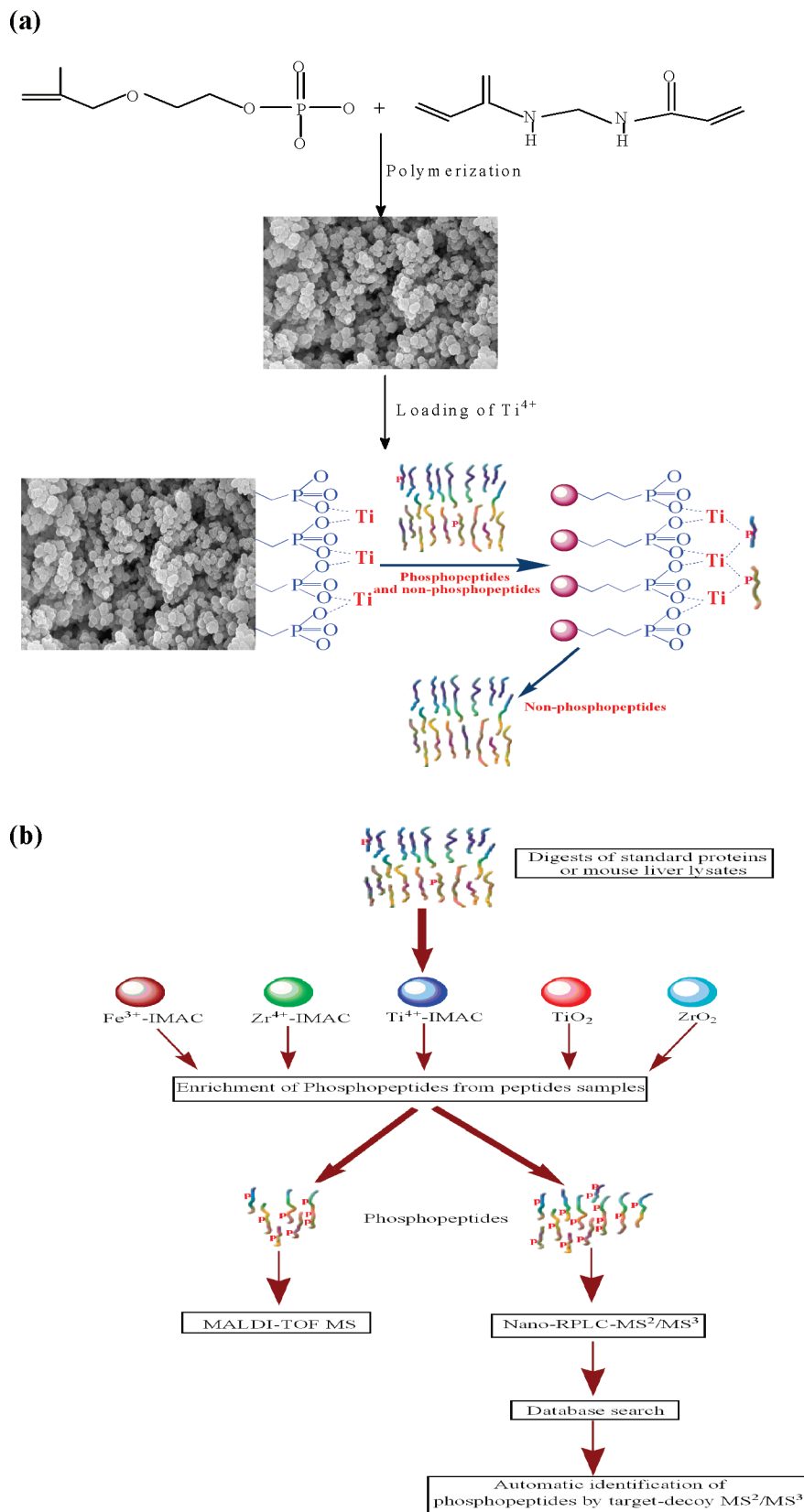
## Experimental Section

**Reagents and Materials.** Proteins of  $\alpha$ -casein,  $\beta$ -casein, bovine serum albumin (BSA), ovalbumin and 1-1-(tosylamido)-2-phenyl-ethyl chloromethylketone (TPCK)-treated trypsin (E.G 2.4.21.4) were purchased from Sigma (St. Louis, MO). Chemical reagents of 2,5-dihydroxybenzoic acid (2,5-DHB),  $\text{ZrOCl}_2$ , trifluoroacetic acid (TFA), ethylene glycol methacrylate phosphate (EGMP), bis-acrylamide (BAA), dimethylsulfoxide, dodecanol, and  $N,N'$ -dimethylformamide were obtained from Sigma (St. Louis, MO). Model singly tyrosine phosphorylated peptide (pY, RRLIEDAEPYAARG, MW 1599) was obtained from Upstate Bio. Co. (NY).  $\text{Ti}(\text{SO}_4)_2$  was obtained from the Sinopharm. Chemical Reagents Co. Ltd. (Shanghai, China). Azobisisobutyronitrile (AIBN) was obtained from Shanghai Fourth Reagent Plant (Shanghai, China). Titanium dioxide ( $\text{TiO}_2$ ) beads were obtained from a disassembled titanium dioxide cartridge purchased from GL Sciences, Inc. (Tokyo, Japan). Zirconium dioxide was prepared as reported in our previous work.<sup>21</sup> Deionized water used for all experiments was purified with a Milli-Q water system (Millipore, Milford, MA). All other reagents and solvents were of the highest commercial quality and were used without further purification. Adult female C57 mice were purchased from Dalian Medical University (Dalian, China).

**Preparation of  $\text{Ti}^{4+}$ -IMAC,  $\text{Zr}^{4+}$ -IMAC, and  $\text{Fe}^{3+}$ -IMAC Beads.** The polymer monolith containing phosphate group were prepared as reported in our previous work.<sup>53</sup> Briefly, the reaction mixtures consisting of EGMP (13% (w/w)), BAA (10% (w/w)), porogenic reagents (77% (w/w)) including dimethylsulfoxide (540  $\mu\text{L}$ ), dodecanol (400  $\mu\text{L}$ ),  $N,N'$ -dimethylformamide (100  $\mu\text{L}$ ), and initiator reagents of AIBN were placed in a tube and sonicated for 20 min to obtain a homogeneous solution, and then purged with nitrogen for 10 min. After sealing, the tube was submerged into a water bath and allowed to react for 12 h at 60 °C. After polymerization, a porous polymer monolith was obtained. Subsequently, the obtained porous polymer monolith was ground into the irregular beads. The polymer beads were extensively washed with methanol for several times, and then they were centrifuged at 20 000g for 2 min, methanol-filtered and dried in vacuum for 2 h. The immobilized  $\text{Ti}^{4+}$  polymer beads ( $\text{Ti}^{4+}$ -IMAC) were obtained by incubation of 10 mg of polymer beads in 100 mM  $\text{Ti}(\text{SO}_4)_2$  solution at room temperature overnight under gentle stirring. The obtained  $\text{Ti}^{4+}$ -IMAC beads were centrifuged at 20 000g for 2 min. After the supernatant was removed, distilled water was used to wash the  $\text{Ti}^{4+}$ -IMAC beads several times to remove the residue titanium ion. The obtained  $\text{Ti}^{4+}$ -IMAC beads were dispersed in 30% ACN containing 0.1% TFA solution before usage. The generation of  $\text{Ti}^{4+}$ -IMAC was shown in Scheme 1a. The  $\text{Zr}^{4+}$ -IMAC were prepared the same as the above protocol of  $\text{Ti}^{4+}$ -IMAC except the incubation of polymer beads was in  $\text{ZrOCl}_2$  solution instead of  $\text{Ti}(\text{SO}_4)_2$  solution.  $\text{Fe}^{3+}$ -IMAC beads (POROS 20 MC beads) were activated according to the manufacturer's instructions by Applied Biosystems Co. Ltd. (Foster, CA).

**Preparation of Peptide Samples.**  $\alpha$ -Casein and  $\beta$ -casein (1 mg) were dissolved in 1 mL of ammonium bicarbonate (50 mM, pH 8.2) and digested for 16 h at 37 °C with trypsin at enzyme-

**Scheme 1.** (a) Schematic Diagram of Preparation of  $Ti$ -IMAC for Phosphopeptide Enrichment; (b) Schematic Diagram Showing the Isolation of Phosphopeptides by Different Methods Followed with MALDI-TOF MS Analysis and Nano-LC-MS<sup>2</sup>/MS<sup>3</sup> Analysis



to-protein ratio of 1:40 (w/w). BSA (6.6 mg) and ovalbumin (4.5 mg) were separately dissolved in 1 mL of denaturing buffer containing 8 M urea and 50 mM ammonium bicarbonate and incubated for 3 h. To the obtained protein solution, 20  $\mu$ L of

50 mM DTT was added and the solution was incubated for 2 h at 37 °C. Then, 40  $\mu$ L of 50 mM IAA was added and the obtained solution was incubated for an additional 30 min at room temperature in the dark. After that, the mixture was diluted by

10-fold with 50 mM ammonium bicarbonate and incubated for 16 h at 37 °C with trypsin at an enzyme/substrate ratio of 1:40 (w/w) to produce proteolytic digests. The obtained peptide solution was lyophilized by a vacuum concentrator for usage.

Peptide mixture 1 contained 1 pmol tryptic digest of  $\alpha$ -casein. Peptide mixture 2 contained peptides originating from a tryptic digests of  $\alpha$ -casein and BSA. Peptide mixture 2 with ratios of 1:100 and 1:500 referred to the peptide mixtures originating from tryptic digests of 1 pmol of  $\alpha$ -casein and 100 pmol of BSA, and 0.2 pmol of  $\alpha$ -casein and 100 pmol of BSA, respectively.

Peptide mixture 3 contained peptides originating from a tryptic digests of  $\beta$ -casein, ovalbumin, BSA and model tyrosine phosphorylated peptide (pY). Peptide mixture 3 (ratio of 1:1:1:500) refers to a mixture of peptides from tryptic digests of 1 pmol of the  $\beta$ -casein, ovalbumin, pY and 500 pmol of the BSA.

The protein extract from the mouse livers was prepared according to procedures described in detail in our previous reports.<sup>4,21</sup> The Bradford protein assay was used to quantify the concentration of the extracted protein. The trypsin digestion of the protein extract was the same as that of BSA and ovalbumin.

**Purification of Phosphopeptides Using  $\text{Ti}^{4+}$ -IMAC and  $\text{Zr}^{4+}$ -IMAC.** The whole procedure for the isolation and analysis of phosphopeptides is shown in Scheme 1b. Peptide mixtures (Peptide mixture 1, 2, or 100  $\mu\text{g}$  of tryptic digests of mouse liver lysate) were first incubated with 5 or 100  $\mu\text{L}$  of  $\text{Ti}^{4+}$ -IMAC or  $\text{Zr}^{4+}$ -IMAC beads (10  $\text{mg}\cdot\text{mL}^{-1}$ ) in loading buffer with vibration of 30 min. The supernatant was removed after centrifugation and the beads with captured phosphopeptides were washed with 30 or 300  $\mu\text{L}$  of two washing buffers, respectively. The bound phosphopeptides were then eluted with 10 or 100  $\mu\text{L}$  of 10%  $\text{NH}_3\cdot\text{H}_2\text{O}$  under sonication for 10 min. After centrifugation at 20 000g for 5 min, the supernatant was collected and lyophilized to dryness. For the phosphopeptides enriched from peptide mixtures 1 and 2, 2  $\mu\text{L}$  of DHB solution (25  $\text{mg}/\text{mL}$  in 70% ACN) containing 1%  $\text{H}_3\text{PO}_4$  (v/v)<sup>54</sup> was added and 0.5  $\mu\text{L}$  of resulting solution was deposited on the MALDI target for MALDI-TOF MS analysis. For the phosphopeptides enriched from mouse liver digests, they were acidified with 0.1% formic acid and subjected to LC-MS<sup>2</sup>/MS<sup>3</sup> analysis.

To optimize the performance of phosphopeptide enrichment, different combinations of loading buffer and washing buffers (which are given in Supplementary Table 1) were tested. Protocol A: 80% ACN, 0.1% TFA as loading buffer, 50% ACN, 0.1% TFA containing 200 mM NaCl as washing buffer 1, and 30% ACN, 0.1% TFA as washing buffer 2. Protocol B: DHB solution (300  $\text{mg}\cdot\text{mL}^{-1}$  in 80% ACN, 0.1% TFA) as loading buffer, 80% ACN, 0.1% TFA containing 300  $\text{mg}\cdot\text{mL}^{-1}$  DHB as washing buffer 1 and 30% ACN, 0.1% TFA as washing buffer 2. Protocol C: 50% ACN containing 10% HAC as loading buffer, 50% ACN, 10% HAC as washing buffer 1 and 0.1% HAC as washing buffer 2. The composition of loading buffer and washing buffer was further optimized based on protocol A. The final optimized protocol (protocol D): 80% ACN, 6% TFA as loading buffer, 50% ACN, 6% TFA containing 200 mM NaCl as washing buffer 1, and 30% ACN, 0.1% TFA as washing buffer 2. If not otherwise stated, protocol D was used for phosphopeptide enrichment by  $\text{Ti}^{4+}$ -IMAC and  $\text{Zr}^{4+}$ -IMAC in this work.

**Purification of Phosphopeptides Using  $\text{TiO}_2$ ,  $\text{ZrO}_2$ , and  $\text{Fe}^{3+}$ -IMAC.** Isolation of phosphopeptides using  $\text{TiO}_2$ : The two protocols, that is, protocols A and B, used for  $\text{Ti}^{4+}$ -IMAC were also applied to isolate phosphopeptides by  $\text{TiO}_2$ .

Isolation of phosphopeptides using  $\text{ZrO}_2$ : The protocol C was also applied to isolate phosphopeptides by  $\text{ZrO}_2$ .

Isolation of phosphopeptides using  $\text{Fe}^{3+}$ -IMAC: Isolation of phosphopeptides by  $\text{Fe}^{3+}$ -IMAC was followed with the optimized protocols recently reported by Lee et al.<sup>29</sup> Briefly, peptide mixture 2 or tryptic digests of mouse liver lysate (100  $\mu\text{g}$ ) were incubated with the 5 or 100  $\mu\text{L}$  of  $\text{Fe}^{3+}$ -IMAC beads (10  $\text{mg}\cdot\text{mL}^{-1}$ ) for 30 min with end-over-end rotation. After that, the beads were washed with 30 or 300  $\mu\text{L}$  washing buffer according to the optimized method. Lastly, the bound peptides were eluted with 10 or 100  $\mu\text{L}$  of 10%  $\text{NH}_3\cdot\text{H}_2\text{O}$ .

In summary, the loading and washing buffers for enrichment of phosphopeptides with different enrichment methods are listed in Supplementary Table 1. The general procedure of phosphopeptide enrichment and identification is outlined in Scheme 1.

**Mass Spectrometry Analysis.** MALDI-TOF mass spectrometry analysis was performed on a Bruker Autoflex time-of-flight mass spectrometer (Bruker, Bremen, Germany). The instrument was equipped with a delayed ion-extraction device and a pulsed nitrogen laser operated at 337 nm and its available accelerating potentials was in the range of  $\pm 20$  kV. The MALDI uses a ground-steel sample target with 384 spots. The range of laser energy was adjusted to slightly above the threshold to obtain good resolution and signal-to-noise ratio (S/N). All mass spectra reported were obtained in the positive ion linear mode with delayed extraction for 90 ns. External mass calibration was obtained by using two points that bracketed the mass range of interest. And each mass spectrum was typically summed with 30 laser shots.

LTQ linear ion trap mass spectrometer (Thermo-electron) with a nanospray source was used with a Finnigan surveyor MS pump (Thermo-electron). The pump flow rate was split by a cross to achieve the flow rate at ca. 200 nL/min. The columns were in-house packed with C18 AQ particles (5  $\mu\text{m}$ , 120 Å) from Michrom BioResources (Auburn, CA) using a pneumatic pump. The separation of phosphopeptides enriched from the tryptic digest of mouse liver lysate was performed using 75 min linear gradient elution. The mobile phase consisted of mobile phase A, 0.1% formic acid in  $\text{H}_2\text{O}$  (v/v), and mobile phase B, 0.1% formic acid in acetonitrile. The LTQ instrument was operated at positive ion mode. A voltage of 1.8 kV was applied to the cross. About 1  $\mu\text{L}$  (20  $\mu\text{g}$ ) of redissolved peptides were loaded onto the C18 capillary column using 75  $\mu\text{m}$  i.d.  $\times$  220 mm length capillary column as a sample loop. The detection of phosphopeptides was performed in which the mass spectrometer was set as a full scan MS followed by three data-dependent MS/MS (MS<sup>2</sup>). Subsequently MS/MS (MS<sup>3</sup>) spectrum was automatically triggered when the 10 most intense peak from the MS<sup>2</sup> spectrum corresponded to a neutral loss event of 98  $m/z$ , 49  $m/z$  and  $33 \pm 1$  Da for the precursor ion with 1+, 2+, and 3+ charge states, respectively.

**Phosphopeptides Identification.** An automatic validation approach developed in-house termed as MS<sup>2</sup>/MS<sup>3</sup> target-decoy search approach was used for phosphopeptide identification by combining the information obtained from MS<sup>2</sup> spectra and its corresponding neutral loss MS<sup>3</sup> spectra.<sup>55</sup> Briefly, there are four steps: (1) evaluation of charge state to remove invalid MS<sup>2</sup>/MS<sup>3</sup> pairs; (2) performing MS<sup>2</sup> and MS<sup>3</sup> target-decoy database searches, separately; (3) reassignment of the peptide scores in SEQUEST output to generate a list of peptide identifications for pair of MS<sup>2</sup>/MS<sup>3</sup> spectra; (4) filtering the candidate phosphopeptides with criteria ( $\text{Rank}'_{\text{m}} = 1$ ,  $\Delta\text{Cn}'_{\text{m}} \geq 0.1$ , and the



Xcorr's cutoff value was determined by increasing its value until the observed FDR was just lower than 1%). The peak lists for  $\text{MS}^2$  and  $\text{MS}^3$  spectra were generated from the raw data by Bioworks v 3.2 (Thermo-electron) with the following parameters: mass range was 600–3500; intensity was 1000; minimum ion count was 10. After removal of invalid  $\text{MS}^2/\text{MS}^3$  pairs, the remaining  $\text{MS}^2$  and  $\text{MS}^3$  were submitted to Sequest database search. The target-decoy database was created by combining original database (ipi.MOUSE.3.21.fasta) and its reversed version. The  $\text{MS}^2$  spectra were searched with a precursor-ion mass tolerance of 2 Da and fragment ion mass tolerance was 1 Da; enzyme set as trypsin and allowance up to two missed cleavages and the static modification was set for alkylation of Cys (+57 Da). For  $\text{MS}^2$  data searching, dynamic modifications were set for oxidized Met (+16), and phosphorylated Ser, Thr and Tyr (+80). For the  $\text{MS}^3$  data searching, besides above settings, dynamic modifications were also set for water loss on Ser, Thr (−18). For all peptides identified by  $\text{MS}^2$ , the following criteria were used: Cross-correlation value (Xcorr)  $\geq 1.9$ , 2.2, 3.75 for single, double, triple charges, and Delta Cn  $\geq 0.1$ .

## Results and Discussion

**Preparation of  $\text{Ti}^{4+}$ -IMAC Absorbents.** It is well-known that self-assembling monolayer and multilayer thin films of phosphate-containing molecules can be formed because of the strong interaction between phosphate groups and  $\text{Ti}^{4+}$  or  $\text{Zr}^{4+}$ .<sup>51,56–58</sup> In the layer structure, the metal ion form stacked planes held together by attractive interactions of the phosphate groups that project into the interlayer region from both sides of any given metal plane. Taking advantage of this strong interaction, we have successfully immobilized  $\text{Zr}^{4+}$  on the poly(glycidyl methacrylate-co-ethylene dimethacrylate) polymer (GMA-EDMA) beads and phosphate modified porous silicon wafer for isolation of phosphopeptides.<sup>4,52</sup> As the interaction between phosphate group and  $\text{Ti}^{4+}$  is also strong,  $\text{Ti}^{4+}$  could be immobilized to the support in the same way. The first step to prepare  $\text{Ti}^{4+}$ -IMAC absorbents is to prepare the beads carrying phosphate groups. The phosphate group modified GMA-EDMA beads<sup>4</sup> could be used to immobilize  $\text{Ti}^{4+}$ . However, preparation of these beads requires multiple chemical derivatization reactions to covalently couple phosphate groups on the surface of GMA-EDMA beads, which is complex and may result in the limited functional groups due to the incompleteness of these reactions. In this work, we synthesized a monolithic polymer containing phosphate groups by direct copolymerization of an ethylene glycol methacrylate phosphate (EGMP) and bis-acrylamide (BAA) in a ternary porogenic solvent consisting of dimethylsulfoxide, dodecanol and *N,N*-dimethylformamide. After polymerization in a tube, a polymer monolith will be formed. Because the monomer, EGMP, contains phosphate group and the phosphate group does not take part in the reaction during polymerization, the obtained polymer also has phosphate groups. The polymer material is hydrophilic and biocompatible due to the usage of hydrophilic cross-linker of bis-acrylamide. Compared with phosphated supports prepared by multiple steps of chemical derivatization, functionalized polymer prepared by direct polymerization can provide more abundance of chelating ligand of phosphate groups. Phosphate polymer beads were prepared by grinding monolithic polymer to obtain irregular beads. The SEM (scanning electron microscope) image of these beads is shown in the Supplementary Figure 1. It was estimated that the size distributions of the ground beads ranged from 1 to 5  $\mu\text{m}$ . Apparently,

the large amount of pores like alveolation were located on the surface of beads. Immobilization of  $\text{Ti}^{4+}$  onto the polymer beads was achieved simply by incubation of the beads in  $\text{Ti}(\text{SO}_4)_2$  solution.  $\text{Ti}^{4+}$  was immobilized via the strong interaction between  $\text{Ti}^{4+}$  and phosphate groups on the surface of polymer beads. The generation of  $\text{Ti}^{4+}$ -IMAC was shown in the Scheme 1a. During the procedure of phosphopeptide enrichment by IMAC, high concentrations of strong acids such as TFA are often included in the loading and washing buffers to protonate the acidic carboxylates residues of peptide to minimize nonspecific adsorption, and alkali solution with extremely high pH is typically used to elute phosphopeptides from beads. The good hydrophilicity, stability, and durability, as well as alkali and acidic resistance of the prepared polymer material, are very suitable for use in phosphopeptide enrichment.

**Enrichment of Phosphopeptides by  $\text{Ti}^{4+}$ -IMAC.** The phosphopeptides could be trapped by  $\text{Ti}^{4+}$ -IMAC via the specific interaction between immobilized  $\text{Ti}^{4+}$  and phosphate group on the phosphopeptides. The procedure for phosphopeptide enrichment by  $\text{Ti}^{4+}$ -IMAC includes three main steps: loading of sample, washing to remove nonspecifically adsorbed peptides and elution of captured phosphopeptides. Tryptic digest of standard protein of  $\alpha$ -casein (peptide mixture 1) was used as the sample to evaluate the ability of  $\text{Ti}^{4+}$ -IMAC for isolation of phosphopeptides. The  $\alpha$ -casein tryptic digest was first dissolved in loading buffer, that is, 50% ACN containing 10% HAC, and then incubated with  $\text{Ti}^{4+}$ -IMAC beads for 30 min. The supernatant was removed after centrifugation. The beads were further washed with a solution including 50% ACN and 10% HAC and a solution including only 50% ACN, respectively. The adsorbed peptides were then eluted by 10%  $\text{NH}_3 \cdot \text{H}_2\text{O}$  for MALDI-TOF MS analysis. The obtained MALDI spectrum is shown in Figure 1a. Only dominant phosphopeptide peaks were observed, which indicated that phosphopeptides could be captured by  $\text{Ti}^{4+}$ -IMAC. The sequences for the phosphopeptides derived from tryptic digest of  $\alpha$ -casein are given in Supplementary Table 2.

Various combinations of loading buffers and washing buffers were used for isolation of phosphopeptides by  $\text{TiO}_2$ .<sup>14–16</sup> The mechanism for isolation of phosphopeptides by  $\text{TiO}_2$  and  $\text{Ti}^{4+}$ -IMAC are similar, which are both based on the interaction between  $\text{Ti}^{4+}$  and phosphate group on phosphopeptide. Therefore, the conditions for phosphopeptide enrichment by  $\text{TiO}_2$  may also be applicable to  $\text{Ti}^{4+}$ -IMAC. Herein, three protocols with different combinations of loading and washing buffers (Supplementary Table 3) were tested for their ability to isolate phosphopeptides by  $\text{Ti}^{4+}$ -IMAC. Protocol A: 80% ACN, 0.1% TFA as loading buffer, 50% ACN, 0.1% TFA containing 200 mM NaCl as washing buffer 1, and 30% ACN, 0.1% TFA as washing buffer 2. Protocol B: DHB solution (300  $\text{mg} \cdot \text{mL}^{-1}$  in 80% ACN, 0.1% TFA) as loading buffer, 80% ACN, 0.1% TFA containing 300  $\text{mg} \cdot \text{mL}^{-1}$  DHB as washing buffer 1 and 30% ACN, 0.1% TFA as washing buffer 2. Protocol C: 50% ACN containing 10% HAC as loading buffer, 50% ACN, 10% HAC as washing buffer 1 and 50% ACN as washing buffer 2. To investigate the specificity of phosphopeptide isolation with different protocols, a relative complex sample, peptide mixture 2 originating from tryptic digests of  $\alpha$ -casein and BSA with ratio of 1:100, was used as the test sample. Spectrum obtained for direct MALDI MS analysis of peptide mixture 2 is shown in Figure 1b. Because the nonphosphopeptides were not removed, nonphosphopeptide peaks dominate the mass spectrum and phosphopeptides cannot be observed. The typical MALDI MS spectra for the

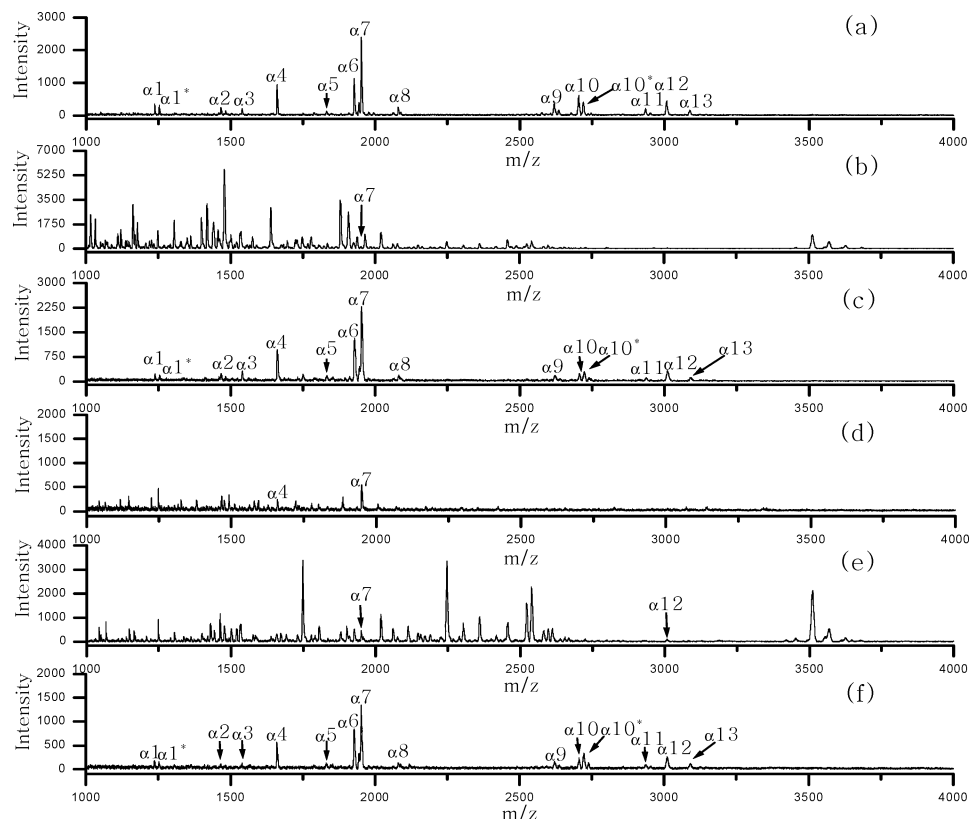


**Figure 1.** MALDI mass spectra for selective enrichment of phosphopeptides by  $\text{Ti}^{4+}$ -IMAC. (a) Phosphopeptides enriched from Peptide mixture 1; (b) direct analysis of Peptide mixture 2 (1:100); (c–e) phosphopeptides enriched from Peptide mixture 2 (1:100) with protocols A (c), B (d) and C (e); (f) phosphopeptides enriched from peptide mixture 2 (1:500) with protocol D. Peptide mixture 1, tryptic digest of  $\alpha$ -casein; peptide mixture 2, the mixture of tryptic digests of  $\alpha$ -casein and BSA with ratio of 1:100 or 1:500. See Supplementary Table 1 for detail conditions.

analysis of phosphopeptides enriched with above three protocols are also shown in the Figures 1c–e. It is obvious that protocol A yields best phosphopeptide enrichment efficiency. We next attempted to further optimize protocol A by changing the concentration of TFA and ACN in loading buffer. When 6% TFA/80% ACN was used as loading buffer, almost all 13 phosphopeptides from peptide mixture 2 were highly selectively enriched with better signal-to-noise ratio than other tested compositions of TFA/ACN (spectrum is not shown). The obtained results demonstrated that high concentration of TFA can efficiently protonate the carboxyl groups so as to prevent nonspecific binding of peptides. This is consistent with the results observed for phosphopeptide enrichment with  $\text{TiO}_2$  by Imanishi et al.<sup>16</sup> In addition to the procedure described by Imanishi et al.,<sup>16</sup> 200 mM NaCl was added into the washing buffer to improve the selectivity in this study. When compared with original washing buffer of 80% ACN/6% TFA, the addition of salt in the washing buffer can greatly improve the enrichment specificity of phosphopeptides by disrupting weak, nonspecific interactions between the  $\text{Ti}^{4+}$ -IMAC beads and polar groups in the amino acid residues.<sup>29</sup> The optimized loading and washing buffer (Protocol D) for enrichment of phosphopeptides by  $\text{Ti}^{4+}$ -IMAC were used in all experiments presented below.

Phosphoproteins are often low-abundance components in real biological protein samples. We further reduced the ratio of tryptic digest of  $\alpha$ -casein in peptide mixture 2 to 1:500 in order to test the performance of  $\text{Ti}^{4+}$ -IMAC to enrich lower abundance phosphopeptides. As shown in Figure 1f, a total of

13 phosphopeptides were clearly presented in the spectrum and signals of phosphopeptides were only slightly reduced even with 500-fold dilution by peptides from nonphosphoprotein of BSA. This indicated that sample complexity and extreme low abundance does not significantly compromise the phosphopeptide enrichment performance of  $\text{Ti}^{4+}$ -IMAC. Specific isolation of phosphopeptides from peptide mixture with 100-fold dilution by nonphosphoprotein of tryptic digests of BSA was reported.<sup>4,21,52</sup> This is the first time for demonstrating that phosphopeptide enrichment approach could specifically isolate phosphopeptides from peptide mixture with 500-fold dilution by peptides from nonphosphorylated proteins.

Because of a lack of phosphorylated tyrosine residues in standard phosphoproteins used in this study, a tyrosine phosphorylated peptide (pY, RRLIEDAEPYAARG, MW 1599) was included in the sample to investigate if  $\text{Ti}^{4+}$ -IMAC can enrich all type of phosphopeptides. Peptide mixture 3 originating from tryptic digestions of ovalbumin (1 pmol),  $\beta$ -casein (1 pmol) and pY (1 pmol) was mixed with tryptic digest of BSA in the ratio of 1:1:1:500. Direct analysis of the peptide mixture 3 by MALDI MS generates spectrum with dominant high-abundance non-phosphopeptides peaks as shown in Figure 2a. The  $\text{Ti}^{4+}$ -IMAC was directly applied to enrich phosphopeptides from the digest mixture without the BSA digest, that is, it only contained digests of 1 pmol ovalbumin, 1 pmol  $\beta$ -casein and 1 pmol pY. The obtained spectrum is shown in the Figure 2b, in which only seven phosphopeptide peaks, that is, O1 and O2 from ovalbumin,  $\beta$ 1,  $\beta$ 2,  $\beta$ 3, and  $\beta$ 4 from  $\beta$ -casein, and the pY, could be clearly observed in the MALDI MS spectrum as shown in Figure

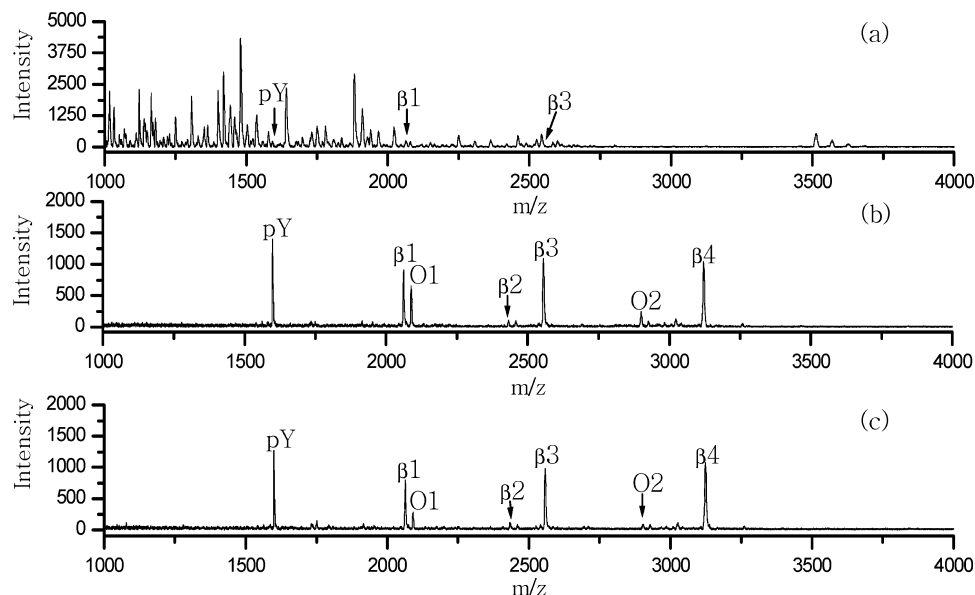


**Figure 2.** MALDI mass spectra for selective enrichment of phosphopeptides by  $\text{Ti}^{4+}$ -IMAC. (a) Direct analysis of peptide mixture 3, (b) analysis of phosphopeptides enriched from the peptide mixture of the digests of  $\beta$ -casein, ovalbumin and pY (no BSA digest); (c) analysis of phosphopeptides enriched from peptide mixture 3. Peptide mixture 3: the mixture of tryptic digests of  $\beta$ -casein, ovalbumin, standard tyrosine phosphorylated peptides (pY) and 500-fold more digest of BSA.

2b. The sequence and phosphorylated sites of the above-mentioned seven phosphopeptides are listed in Supplementary Table 2. However, after phosphopeptide enrichment by  $\text{Ti}^{4+}$ -IMAC in the presence of 500-fold BSA digests, the same seven phosphopeptides including pY dominated the MS spectrum with almost equivalent peak intensity. This indicated that very low abundance phosphopeptides could be effectively enriched even with 500-fold dilution by nonphosphoprotein of the BSA. Peptides phosphorylation on serine, threonine, and tyrosine residues were all enriched which demonstrated there was no bias for enrichment of different type of phosphopeptides by  $\text{Ti}^{4+}$ -IMAC. Urea, DTT and IAA are often introduced into proteolysis digestions of biological sample. Urea was essential for denaturing ovalbumin and BSA. Meanwhile, DTT was added to open the disulfide bond and IAA was added to carbamidomethylate the resulting cysteine residues. There were 200  $\mu\text{M}$  of DTT, 400  $\mu\text{M}$  of IAA and 1.6 M of urea presented in the final solution of peptide mixture 3. The excellent performance for isolation of phosphopeptides from peptide mixture 3 indicated the presence of these interferential substances hardly compromised the specificity of phosphopeptide enrichment by  $\text{Ti}^{4+}$ -IMAC.

**Comparing the Performance of  $\text{Ti}^{4+}$ -IMAC with Other Methods Using Semicomplex Sample.** By far, several methods have been developed for enrichment of phosphopeptides based on the different types of adsorbents. To demonstrate the performance of  $\text{Ti}^{4+}$ -IMAC, it was compared with  $\text{Zr}^{4+}$ -IMAC,  $\text{Fe}^{3+}$ -IMAC,  $\text{TiO}_2$  and  $\text{ZrO}_2$  for the isolation of phosphopeptides. As the specific isolation of phosphopeptides from peptide mixture with 500-fold dilution by peptides from nonphosphoprotein is challenging, peptide mixture 2 (ratio, 1:500) was used as semicomplex sample to investigate their performance. The used conditions for each method were listed in Supplementary Table 1. After the enrichment, the resulting phosphopeptides were analyzed by MALDI MS.

First,  $\text{Fe}^{3+}$ -IMAC, which is still widely used for isolation of phosphopeptides, was tested. Purification of phosphopeptides by  $\text{Fe}^{3+}$ -IMAC was followed with the optimal strategy recently

described by Lee et al.<sup>29</sup> The obtained MALDI spectrum is shown in Figure 3a. Compared with the spectrum in Figure 1c obtained by  $\text{Ti}^{4+}$ -IMAC, the  $\text{Fe}^{3+}$ -IMAC method lacks enough specificity and results in many signals of nonphosphopeptides. Only a few multiply phosphorylated peptides ( $\alpha 9$ ,  $\alpha 10$  and  $\alpha 12$ ) were observed and the signals of the singly phosphorylated peptides, for example,  $m/z$  1660.79, 1951.95, were not observed (Figure 3a). It is obvious that  $\text{Fe}^{3+}$ -IMAC showed a preferential enrichment of multiply phosphorylated peptides. Similar results were also observed in previous works.<sup>14,47,59</sup> The loss of singly phosphorylated peptide is probably because the interaction between phosphopeptides and  $\text{Fe}^{3+}$ -IMAC adsorbents is too weak. Significantly large number of nonphosphopeptides was observed in the spectrum, which indicated the  $\text{Fe}^{3+}$ -IMAC lack enough specificity.

Previously, we have demonstrated that  $\text{Zr}^{4+}$ -IMAC has high specificity for isolation of phosphopeptides from semicomplex mixtures as well as real biological samples.<sup>4,52</sup> Instead of using EDMA-GMA beads, the  $\text{Zr}^{4+}$ -IMAC adsorbents used in this study was also made from the phosphate polymer beads as that of  $\text{Ti}^{4+}$ -IMAC.  $\text{Zr}^{4+}$  was immobilized by incubating the phosphate polymer beads in  $\text{ZrOCl}_2$  solution. The optimization procedures for isolation of phosphopeptides by  $\text{Zr}^{4+}$ -IMAC was followed with the same strategy for  $\text{Ti}^{4+}$ -IMAC. The MALDI spectrum for analysis of phosphopeptides enriched by  $\text{Zr}^{4+}$ -IMAC under optimal condition is shown in Figure 3b. It is obvious that the seven phosphopeptides ( $\alpha 4$ ,  $\alpha 6$ ,  $\alpha 7$ ,  $\alpha 8$ ,  $\alpha 9$ ,  $\alpha 10$  and  $\alpha 12$ ) were also specifically enriched. It can be seen from Figure 1f and Figure 3b that both  $\text{Ti}^{4+}$ -IMAC and  $\text{Zr}^{4+}$ -IMAC show high specificity for isolation of phosphopeptides. However, it should be noted that the relative intensity of singly versus multiply phosphopeptides was different between  $\text{Ti}^{4+}$ -IMAC and  $\text{Zr}^{4+}$ -IMAC. It was found that single phosphopeptides were being enriched to a higher extent with  $\text{Ti}^{4+}$ -IMAC. The strongest signal following  $\text{Ti}^{4+}$ -IMAC enrichment originates from the singly phosphorylated peptide (YKVPQLEIVNPp-SAEER) at  $m/z$  1951.95 corresponded to  $\alpha 7$  as shown in the Figure 1c,f. In contrast, the doubly phosphorylated peptides

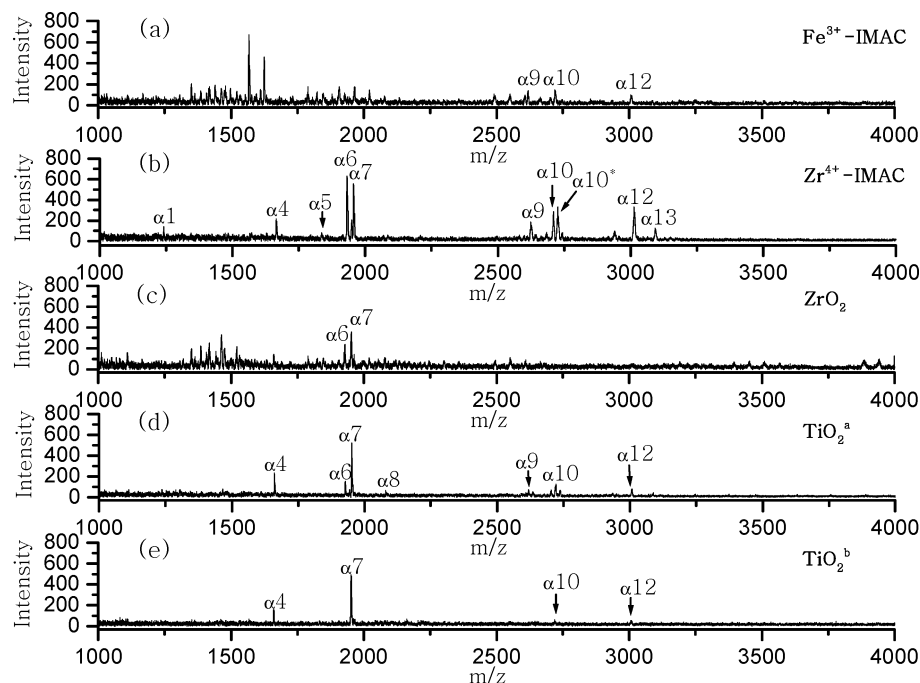


**Figure 3.** MALDI mass spectra for analysis of phosphopeptides enriched from the peptide mixtures of tryptic digests of  $\alpha$ -casein and BSA with ratio of 1:500 by different adsorbents. (a)  $\text{Fe}^{3+}$ -IMAC; (b)  $\text{Zr}^{4+}$ -IMAC; (c)  $\text{ZrO}_2$ ; (d)  $\text{TiO}_2$  with TFA included in loading and washing buffers; (e)  $\text{TiO}_2$  with DHB included in loading and washing buffers. Refer to Supplementary Table 1 for detail conditions.

(DIGpSepSTEDQAMEDIK) at  $m/z$  1927.69 corresponded to  $\alpha 6$  is the most abundant peak following  $\text{Zr}^{4+}$ -IMAC enrichment as shown in the Figure 3b.  $\text{Zr}^{4+}$ -IMAC tends to enrich multiply phosphorylated peptides probably because the binding of singly phosphorylated peptides are weak. This is in accordance to the results of analyzing the semicomplex mixture of tryptic digests of  $\alpha$ -casein or  $\beta$ -casein and BSA with the ratio of 1:100 using the  $\text{Zr}^{4+}$ -IMAC based on GMA-EDMA beads and porous silicon chip.<sup>4,52</sup>

Besides IMAC method, metal oxides such as  $\text{TiO}_2$  and  $\text{ZrO}_2$  particles also have been developed as adsorbent materials to selectively isolate phosphopeptides from complex peptide mixtures because analytes possessing phosphate groups can bridge onto the surface of metal oxide particles. Monodentate, bidentate, and bidentate-bridging phosphate coordination to metal ions are all possible modes involved in such self-assembly process. It was found that these metal oxides had higher selectivity than conventional  $\text{Fe}^{3+}$ -IMAC beads.<sup>14,16,20,23</sup> We next compared the phosphopeptide enrichment performance of  $\text{Ti}^{4+}$ -IMAC with these metal oxides. Peptide mixture 2 (1:500) was pretreated with  $\text{ZrO}_2$  adsorbent followed with the optimal protocol in our previous work.<sup>21</sup> Only two phosphopeptides and large number of nonphosphopeptides were observed in the MALDI spectrum shown in the Figure 3c. It is clear that the phosphopeptide selectivity of  $\text{ZrO}_2$  is not as good as that of  $\text{Ti}^{4+}$ -IMAC and  $\text{Zr}^{4+}$ -IMAC. For phosphopeptide enrichment with  $\text{TiO}_2$  adsorbent, in protocol reported by Imanishi et al.,<sup>16</sup> high concentration of TFA was used to minimize nonspecific adsorption by more efficiently protonating the acidic carboxylates residues of peptide during the loading and washing procedures. Peptide mixture 2 (ratio, 1:500) was incubated with  $\text{TiO}_2$  beads in 80% ACN/6% TFA solution. After washing in turn with 50% ACN/6% TFA containing 200 mM NaCl, 30% ACN/0.1% TFA, the adsorbed phosphopeptides were eluted by 10%  $\text{NH}_3 \cdot \text{H}_2\text{O}$ . The obtained MALDI spectrum is shown in Figure 3d and abundant signals

of phosphopeptides were detected. However, only seven phosphopeptides were detected, and some phosphopeptides ( $\alpha 1$ ,  $\alpha 2$ ,  $\alpha 3$ ,  $\alpha 5$ ,  $\alpha 11$  and  $\alpha 13$ ) were not observed. With another protocol reported by Larsen et al.,<sup>14,15</sup> peptide mixture 2 (ratio, 1:500) was pretreated with  $\text{TiO}_2$  beads using DHB solution for loading samples as well as subsequent washing of the  $\text{TiO}_2$  beads. The obtained MALDI spectrum is shown in Figure 3e, where two singly phosphorylated peptides ( $\alpha 4$  (VPQLEIVNP- $\text{SAEER}$ ,  $m/z$  1660.79) and  $\alpha 7$  (YKVPQLEIVNP- $\text{SAEER}$ ,  $m/z$  1951.95)) and two multiply phosphorylated peptides (QME-AEpSlpSpSpSEEVNPNPpSVEQK,  $m/z$  2719.90, and NANEEY-SIGpSpSpSEEpSAEVATEEVK,  $m/z$  3087.99) were observed. On the basis of the above results, it can be seen that metal oxide particles ( $\text{ZrO}_2$  and  $\text{TiO}_2$ ) cannot compete with  $\text{Ti}^{4+}$ -IMAC and  $\text{Zr}^{4+}$ -IMAC for the isolation of phosphopeptides. One of the possible reasons for poor phosphopeptide enrichment performance of metal oxide particles may be due to the fact that there is no spacer arm and so the presence of steric hindrance obstructs the access of phosphopeptides.

Above experiments demonstrated that  $\text{Ti}^{4+}$ -IMAC had higher specificity than other methods did. We next investigated their performance to enrich low concentration of phosphopeptides.  $\text{Ti}^{4+}$ -IMAC was applied to enrich phosphopeptides from the tryptic digest of  $\alpha$ -casein ( $5 \times 10^{-9}$  M, 10  $\mu\text{L}$ ), whereas only 7 phosphopeptides ( $\alpha 4$ ,  $\alpha 5$ ,  $\alpha 6$ ,  $\alpha 7$ ,  $\alpha 8$ ,  $\alpha 10$  and  $\alpha 12$ ) were detected after MALDI MS analysis (Supplementary Figure 2a). When the concentration of the digest was decreased by 1 order of magnitude (to  $5 \times 10^{-10}$  M, 10  $\mu\text{L}$ ), phosphopeptides of  $\alpha 7$ ,  $\alpha 8$  and  $\alpha 12$  remained observable (Supplementary Figure 2b). If the amount of phosphopeptides enabled the detection of minimum of three phosphopeptides was defined as the detection limitation, the detection limit by the MALDI MS analysis with  $\text{Ti}^{4+}$ -IMAC enrichment was close to 5 fmol. The detection limitations with  $\text{Fe}^{3+}$ -IMAC and  $\text{TiO}_2$  were also determined and they were about 10 times higher than those of  $\text{Ti}^{4+}$ -IMAC beads, which are both close to 50 fmol (Supplementary



**Table 1.** Overview of the Results for Phosphoproteome Analysis of Mouse Liver with Different Methods<sup>a</sup>

method	no. of identified phosphopeptides and distribution of singly, doubly, and triply phosphorylated peptides				no. of identified phosphorylated sites	no. of identified phosphoproteins	phosphopeptide ratio <sup>a</sup>
	total	singly	doubly	triply			
Fe <sup>3+</sup> -IMAC	47	12 (27.7%)	11 (23.4%)	24 (48.9%)	106	37	0.113
TiO <sub>2</sub>	102	82 (79.2%)	16 (16.8%)	4 (4%)	126	70	0.241
ZrO <sub>2</sub>	95	65 (68.4%)	22 (23.2%)	8 (8.4%)	133	71	0.237
Zr <sup>4+</sup> -IMAC	185	147 (79.5%)	31 (16.8%)	7 (3.7%)	230	132	0.476
Ti <sup>4+</sup> -IMAC	216	185 (85.6%)	27 (12.5%)	4 (1.9%)	251	156	0.561

<sup>a</sup> The ratio refers to the number of identified phosphopeptides to number of all identified peptide.

Figure 3). The lower detection limit of  $Ti^{4+}$ -IMAC may arise from the strong affinity and high specificity between the phosphopeptides and  $Ti^{4+}$ -IMAC beads. When using  $Zr^{4+}$ -IMAC and  $ZrO_2$  nanoparticles to selectively trap phosphopeptides from tryptic digest of  $\alpha$ -casein ( $5 \times 10^{-10}$  M, 10  $\mu$ L), three phosphopeptides  $\alpha_4$ ,  $\alpha_6$  and  $\alpha_7$  still can both be detected (Supplementary Figure 4). Thus, the detection limitation for the two techniques was also close to 5 fmol. The strong interaction between the  $Zr^{4+}$ -IMAC and phosphopeptides and the higher specific surface area of  $ZrO_2$  nanoparticles may contribute to enrich and detect phosphopeptides at the femtomole range, respectively. Though 3 phosphopeptides were detected at concentration of  $5 \times 10^{-10}$  M for  $Zr^{4+}$ -IMAC and  $ZrO_2$  nanoparticles, only the same three phosphopeptides were detected at concentration of  $5 \times 10^{-9}$  M (Supplementary Figure 4). However, 7 phosphopeptides could be detected for  $Ti^{4+}$ -IMAC at this concentration ( $5 \times 10^{-9}$  M). Thus,  $Ti^{4+}$ -IMAC could bind more type of phosphopeptides at low concentration.

**Comparing the Performance of  $Ti^{4+}$ -IMAC with Other Enrichment Methods for Phosphoproteome Analysis of Mouse Liver.** The previous results show that  $Ti^{4+}$ -IMAC can be used to effectively isolate and enrich phosphopeptides from relative simple peptide mixtures. We further tested its performance using real complex sample of tryptic digests of mouse liver lysate. A 100  $\mu$ g mouse liver lysate digest was submitted to  $Ti^{4+}$ -IMAC purification followed with the optimized protocol D. The  $Ti^{4+}$ -IMAC-enriched phosphopeptides were analyzed using nano-LC-MS<sup>2</sup>/MS<sup>3</sup> with data-dependent mode. For comparison, 100  $\mu$ g of mouse liver lysate digests were also treated by other methods with enrichment by different adsorbents of Fe<sup>3+</sup>-IMAC,  $Zr^{4+}$ -IMAC, TiO<sub>2</sub> and  $ZrO_2$ . One-fifth of the enriched phosphopeptides was loaded onto capillary C18 column and analyzed by LTQ mass spectrometer. Three replicates of phosphopeptide enrichment and nano-LC-MS<sup>2</sup>/MS<sup>3</sup> runs were conducted for each method. For objectively comparing the performance of phosphopeptide enrichment by every method, an automatic phosphopeptide validation approach (MS<sup>2</sup>/MS<sup>3</sup> target-decoy database search approach) was applied to confirm the identification of phosphopeptides and phosphorylated sites without any manual validation stage.<sup>49</sup> The final analysis results were summarized in Table 1.

The numbers of identified phosphopeptides by  $Ti^{4+}$ -IMAC,  $Zr^{4+}$ -IMAC, TiO<sub>2</sub>,  $ZrO_2$  and Fe<sup>3+</sup>-IMAC were 216, 185, 102, 95 and 47, respectively. Obviously,  $Ti^{4+}$ -IMAC yielded the best results and  $Zr^{4+}$ -IMAC yielded the second best results. The

numbers of identified phosphopeptides by metal oxide particles (TiO<sub>2</sub> and  $ZrO_2$ ) were about 50% of that by IMAC with  $Ti^{4+}$  and  $Zr^{4+}$ . The poorest one, Fe<sup>3+</sup>-IMAC, can only identify about 20% of that  $Ti^{4+}$ -IMAC did. To compare their specificity, the ratio of the number of identified phosphopeptides versus the number of all identified peptides (termed as phosphopeptide ratio) was determined and given in Table 1. The order of this percentage was the same as the number of identified phosphopeptides, that is,  $Ti^{4+}$ -IMAC >  $Zr^{4+}$ -IMAC > TiO<sub>2</sub> >  $ZrO_2$  > Fe<sup>3+</sup>-IMAC. The highest phosphopeptide ratio was obtained for  $Ti^{4+}$ -IMAC which indicated it had the highest specificity for enrichment of phosphopeptides. Compared with multiply phosphorylated peptides, singly phosphorylated peptides are most likely lost during enrichment process because of their weak interaction. So the percentages of identified singly phosphorylated peptides may be a good indicator of the strength of the binding. The percentages of singly phosphorylated peptides identified by the five methods were also given in Table 1. The order was as follows:  $Ti^{4+}$ -IMAC > TiO<sub>2</sub> >  $Zr^{4+}$ -IMAC >  $ZrO_2$  > Fe<sup>3+</sup>-IMAC. This order was quite consistent with the MALDI MS analysis of phosphopeptides enriched from semicomplex sample by these methods.  $Ti^{4+}$ -IMAC had the highest percentage and so the best specificity for interaction between phosphopeptides and the adsorbents. Fe<sup>3+</sup>-IMAC had lowest percentage probably because some singly phosphopeptides were not captured due to the weak interaction. On the basis of above analysis, there are two reasons to account for the high performance of  $Ti^{4+}$ -IMAC for phosphoproteome analysis. The first one is its high specificity. Because of its high specificity, a low percentage of nonphosphopeptides is presented in the enriched samples. Thus, the suppression by nonphosphopeptides during LC-MS<sup>2</sup>/MS<sup>3</sup> analysis is not so serious. The second reason is its strong interaction. Less phosphopeptides were lost during the enrichment process because of the strong interaction, and so more phosphopeptides could be finally identified. Aebersold et al. reported different phosphopeptide isolation methods could detect different, partially overlapping segments of the phosphoproteome.<sup>47</sup> We also found that the overlap of the phosphopeptides identified by these five methods was very low. Only 16 phosphopeptides were identified by all these methods, which demonstrated their complementarities in phosphoproteome analysis. The complete lists of the phosphopeptides identified by these five methods were given in the Supporting Information 2.

## Conclusions

A new type of IMAC adsorbent, that is,  $\text{Ti}^{4+}$ -IMAC, was developed to enrich phosphopeptides for phosphoproteome analysis. Its high specificity and efficiency for purification of phosphopeptides was demonstrated by MALDI MS analysis of phosphopeptides in semicomplex peptide mixture and by LC-MS<sup>2</sup>/MS<sup>3</sup> analysis of mouse liver phosphoproteome. Its performance was comprehensively compared with four other phosphopeptide isolation methods based on the different adsorbents including  $\text{Fe}^{3+}$ -IMAC,  $\text{Zr}^{4+}$ -IMAC,  $\text{TiO}_2$  and  $\text{ZrO}_2$ , and found that  $\text{Ti}^{4+}$ -IMAC had the best performance and  $\text{Fe}^{3+}$ -IMAC had the worst. For  $\text{Ti}^{4+}$ -IMAC and  $\text{Zr}^{4+}$ -IMAC based methods, a conclusion could be drawn: immobilized metal ions ( $\text{Ti}^{4+}$ -IMAC and  $\text{Zr}^{4+}$ -IMAC) have better performance than corresponding metal oxides ( $\text{TiO}_2$  and  $\text{ZrO}_2$ ). This was because the presence of spacer arm in IMAC reduced the steric hindrance which facilitated the binding of phosphopeptides.

Instead of using NTA or IDA, phosphate groups were used as the ligands to immobilize  $\text{Ti}^{4+}$  in this study. To prepare adsorbents with phosphate groups, direct polymerization of monomer with phosphate group to form the polymer monolith was presented. Compared with phosphated supports prepared by multiple steps of chemical derivatization, functionalized polymer prepared by direct polymerization can provide more abundance of chelating ligand of phosphate groups.  $\text{Ti}^{4+}$ -IMAC beads prepared in this study have both the high specificity of titanium ion and good biocompatibility such as hydrophilicity and chemical stability provided by the polymer material.

**Acknowledgment.** Financial supports from the National Natural Sciences Foundation of China (No. 20675081, 20735004), the China State Key Basic Research Program Grant (2005CB522701, 2007CB914102), the China High Technology Research Program Grant (2006AA02A309), the Knowledge Innovation program of CAS (KJCX2.YW.HO9, KSCX2-YW-R-079) and the Knowledge Innovation program of DICP to H.Z. and National Natural Sciences Foundation of China (No. 20605022, 90713017) to M.Y. are gratefully acknowledged.

**Supporting Information Available:** The supplementary data include supplemental Tables 1–3 and supplementary Figures 1–4 in Supporting Information 1 and a list of the phosphopeptides identified by different enrichment method, together with Dcn'm, Xcorr's and site of phosphorylation in Supporting Information 2. This material is available free of charge via the Internet at <http://pubs.acs.org>.

## References

- Walsh, G. T.; Garneau-Tsodikova, S.; Ganto, G. J. *Angew. Chem., Int. Ed.* **2005**, *44*, 7342–7372.
- Pawson, T. *Cell* **2004**, *116*, 191–203.
- Zolnierowicz, S.; Bollen, M. *EMBO J.* **2000**, *19*, 483–488.
- Feng, S.; Ye, M.; Zhou, H.; Jiang, X.; Jiang, X.; Zou, H.; Gong, B. *Mol. Cell. Proteomics* **2007**, *6*, 1656–1665.
- Paradela, A.; Albar, J. P. *J. Proteome Res.* **2008**, *7*, 1809–1818.
- Mann, M.; Jensen, O. N. *Nat. Biotechnol.* **2003**, *21*, 172–177.
- Aebersold, R.; Mann, M. *Nature* **2003**, *422*, 198–207.
- McLachlin, D. T.; Chait, B. T. *Curr. Opin. Chem. Biol.* **2001**, *5*, 591–602.
- Rush, J.; Moritz, A.; Lee, K. A.; Guo, A.; Goss, V. L.; Spek, E. J.; Zhang, H.; Zha, X. M.; Polakiewicz, R. D.; Comb, M. J. *Nat. Biotechnol.* **2005**, *23*, 94–101.
- Hinsby, A. M.; Olsen, J. V.; Mann, M. *J. Biol. Chem.* **2004**, *279*, 46438–46447.
- McLachlin, D. T.; Chait, B. T. *Anal. Chem.* **2003**, *75*, 6826–6836.
- Tao, W. A.; Wollscheid, B.; O'Brien, R.; Eng, J. K.; Li, X. J.; Bodenmiller, B.; Watts, J. D.; Hood, L.; Aebersold, R. *Nat. Methods* **2005**, *2*, 591–598.
- Oda, Y.; Nagasu, T.; Chait, B. T. *Nat. Biotechnol.* **2001**, *19*, 379–382.
- Larsen, M. R.; Thingholm, T. E.; Jensen, O. N.; Roepstorff, P.; Jorgensen, T. J. *Mol. Cell. Proteomics* **2005**, *4*, 873–886.
- Thingholm, T. E.; Jorgensen, T. J.; Jensen, O. N.; Larsen, M. R. *Nat. Protoc.* **2006**, *1*, 1929–1935.
- Imanishi, S. Y.; Kochin, V.; Ferraris, S. E.; de Thonel, A.; Pallari, H. M.; Corthals, G. L.; Eriksson, J. E. *Mol. Cell. Proteomics* **2007**, *6*, 1380–1391.
- Cantin, G. T.; Shock, T. R.; Park, S. K.; Madhani, H. D.; Yates, J. R., III. *Anal. Chem.* **2007**, *79*, 4666–4673.
- Chen, C. T.; Chen, Y. C. *Anal. Chem.* **2005**, *77*, 5912–5919.
- Lin, H. Y.; Chen, C. T.; Chen, Y. C. *Anal. Chem.* **2006**, *78*, 6873–6878.
- Kweon, H. K.; Hakansson, K. *Anal. Chem.* **2006**, *78*, 1743–1749.
- Zhou, H.; Tian, R.; Ye, M.; Xu, S.; Feng, S.; Pan, C.; Jiang, X.; Li, X.; Zou, H. *Electrophoresis* **2007**, *28*, 2201–2215.
- Wolschin, F.; Wienkoop, S.; Weckwerth, W. *Proteomics* **2005**, *5*, 4389–4397.
- Sugiyama, N.; Masuda, T.; Shinoda, K.; Nakamura, A.; Tomita, M.; Ishihama, Y. *Mol. Cell. Proteomics* **2007**, *6*, 1103–1109.
- Li, Y.; Leng, T.; Lin, H.; Deng, C.; Xu, X.; Yao, N.; Yang, P.; Zhang, X. *J. Proteome Res.* **2007**, *6*, 4498–4510.
- Li, X.; Gerber, S. A.; Rudner, A. D.; Beausoleil, S. A.; Haas, W.; Villén, J.; Elias, J. E.; Gygi, S. P. *J. Proteome Res.* **2007**, *6*, 1190–1197.
- Kim, J. E.; Tannenbaum, S. R.; White, F. M. *J. Proteome Res.* **2005**, *4*, 1339–1346.
- Tan, F.; Zhang, Y.; Mi, W.; Wang, J.; Wei, J.; Cai, Y.; Qian, X. *J. Proteome Res.* **2008**, *7*, 1078–1087.
- Posewitz, M. C.; Tempst, P. *Anal. Chem.* **1999**, *71*, 2883–2892.
- Lee, J.; Xu, Y.; Chen, Y.; Sprung, R.; Kim, S. C.; Xie, S.; Zhao, Y. *Mol. Cell. Proteomics* **2007**, *6*, 669–676.
- Li, Y. C.; Lin, Y. S.; Tsai, P. J.; Chen, C. T.; Chen, W. Y.; Chen, Y. C. *Anal. Chem.* **2007**, *79*, 7519–7525.
- Ibanez, A. J.; Muck, A.; Svatos, A. J. *J. Proteome Res.* **2007**, *6*, 3842–3848.
- Blacken, G. R.; Volny, M.; Vaisar, T.; Sadilek, M.; Turecek, F. *Anal. Chem.* **2007**, *79*, 5449–5456.
- Lim, K. B.; Kassel, D. B. *Anal. Biochem.* **2006**, *354*, 213–219.
- Nuhse, T. S.; Stensballe, A.; Jensen, O. N.; Peck, S. C. *Mol. Cell. Proteomics* **2003**, *2*, 1234–1243.
- Villén, J.; Beausoleil, S. A.; Gerber, S. A.; Gygi, S. P. *Proc. Natl. Acad. Sci. U.S.A.* **2007**, *104*, 1488–1493.
- Beausoleil, S. A.; Jedrychowski, M.; Schwartz, D.; Elias, J. E.; Villén, J.; Li, J.; Cohn, M. A.; Cantley, L. C.; Gygi, S. P. *Proc. Natl. Acad. Sci. U.S.A.* **2004**, *101*, 12130–12135.
- Pan, C.; Ye, M.; Liu, Y.; Feng, S.; Jiang, X.; Han, G.; Zhu, J.; Zou, H. *J. Proteome Res.* **2006**, *5*, 3114–3124.
- Blacken, G. R.; Gelb, M. H.; Turecek, F. *Anal. Chem.* **2006**, *78*, 6065–6073.
- Dunn, J. D.; Watson, J. T.; Bruening, M. L. *Anal. Chem.* **2006**, *78*, 1574–1580.
- Neville, D. C.; Rozanas, C. R.; Price, E. M.; Gruis, D. B.; Verkman, A. S.; Townsend, R. R. *Protein Sci.* **1997**, *6*, 2436–2445.
- Loyet, K. M.; Stults, J. T.; Arnott, D. *Mol. Cell. Proteomics* **2005**, *4*, 235–245.
- Ficarro, S. B.; McClelland, M. L.; Stukenberg, P. T.; Burke, D. J.; Ross, M. M.; Shabanowitz, J.; Hunt, D. F.; White, F. M. *Nat. Biotechnol.* **2002**, *20*, 301–305.
- Xu, C. F.; Lu, Y.; Ma, J.; Mohammadi, M.; Neubert, T. A. *Mol. Cell. Proteomics* **2005**, *4*, 809–818.
- Xu, C. F.; Wang, H.; Li, D.; Kong, X. P.; Neubert, T. A. *Anal. Chem.* **2007**, *79*, 2007–2014.
- Moser, K.; White, F. M. *J. Proteome Res.* **2006**, *5*, 98–104.
- Naoyuki, S.; Takeshi, M.; Kosaku, S.; Akihiro, N.; Masaru, T.; Yasushi, I. *Mol. Cell. Proteomics* **2007**, *6*, 1103–1109.
- Bodenmiller, B.; Mueller, L. N.; Mueller, M.; Domon, B.; Aebersold, R. *Nat. Methods* **2007**, *4*, 231–237.
- Yu, L.-R.; Zhu, Z.; Chan, K. C.; Issaq, H. J.; Dimitrov, D. S.; Veenstra, T. D. *J. Proteome Res.* **2006**, *5*, 4150–4162.
- Jiang, W.; Quazi, S.; Wei, L.; Alwin, S.; Follettie, M. T. *J. Proteome Res.* **2007**, *6*, 4684–4689.
- Stanghellini, P. L.; Boccaleri, E.; Diana, E.; Alberti, G.; Vivani, R. *Inorg. Chem.* **2004**, *43*, 5698–5703.
- Nonglaton, G.; Benitez, I. O.; Guisle, I.; Pipelier, M.; Leger, J.; Dubreuil, D.; Tellier, C.; Talham, D. R.; Bujoli, B. *J. Am. Chem. Soc.* **2004**, *126*, 1497–1502.

- (52) Zhou, H.; Xu, S.; Ye, M.; Feng, S.; Pan, C.; Jiang, X.; Li, X.; Han, G.; Fu, Y.; Zou, H. *J. Proteome Res.* **2006**, *5*, 2431–2437.
- (53) Dong, J.; Zhou, H.; Wu, R.; Ye, M.; Zou, H. *J. Sep. Sci.* **2007**, *30*, 2917–2923.
- (54) Kjellstrom, S.; Jensen, O. N. *Anal. Chem.* **2004**, *76*, 5109–5117.
- (55) Jiang, X.; Ye, M.; Han, G.; Feng, S.; Jiang, X.; Yao, X.; Zou, H. *J. Proteome Res.* **2008**, *7*, 1640–1649.
- (56) Wang, Q.; Zhang, L.; Qiu, L.; Sun, J.; Shen, J. *Langmuir* **2007**, *23*, 6084–6090.
- (57) Vasylyev, M. V.; Wachtel, E. J.; Popovitz-Biro, R.; Neumann, R. *Chemistry* **2006**, *12*, 3507–3514.
- (58) Wang, Q.; Zhong, L.; Sun, J.; Shen, J. *Chem. Mater.* **2005**, *17*, 3563–3569.
- (59) Zhang, X.; Ye, J.; Jensen, O. N.; Roepstorff, P. *Mol. Cell. Proteomics* **2007**, *6*, 2032–2042.

PR800223M